Available online at www.sciencedirect.com
ScienceDirect
European Journal of Pharmaceutics and Biopharmaceutics 64 (2006) 238–245
European Journal of Pharmaceutics and Biopharmaceutics
www.elsevier.com/locate/ejpb

Research paper

Distribution characteristics of orally administered olamufloxacin, a newly synthesized fluoroquinolone antibacterial, in lung epithelial lining fluid and alveolar macrophage in rats

Jin Sun [a,b], Yoshiharu Deguchi [a,c], Yoshihiko Tauchi [a], Zhonggui He [b], Gang Cheng [b], Kazuhiro Morimoto [a,*]

[a] Department of Pharmaceutics, Hokkaido Pharmaceutical University, Otaru-city, Hokkaido, Japan
[b] Department of Pharmaceutics, School of Pharmacy, Shenyang Pharmaceutical University, Shenyang, China
[c] Department of Drug Disposition and Pharmacokinetics, School of Pharmaceutical Sciences, Teikyo University, Kanagawa, Japan

Received 25 November 2005; accepted in revised form 20 April 2006
Available online 23 June 2006

Abstract

This study described distribution characteristics of olamufloxacin (HSR-903) in lung epithelial lining fluid (ELF) and alveolar macrophage (AM) in rats, two important representative infectious sites in lower respiratory tract infections. The rats were orally administered at a dose of 10 mg/kg. At each designated time, rats were sacrificed, and blood samples were collected from the superior vena cava, and ELF and AM samples were gathered by the bronchoalveolar lavage method. The AUC ratios of ELF/plasma and AM/plasma of HSR-903 were 3.03 ± 0.54 and 97.5 ± 24.2, respectively, notably higher than those of ciprofloxacin (CPFX). Kinetic analyses of concentration–time profiles of HSR-903 in ELF and AM indicated that the influx clearance from plasma to ELF across the alveolar barrier was 5.8-fold higher than the efflux clearance from ELF. Furthermore, the permeability of HSR-903 across the cultured AM plasma membrane was 5.5 and 14.5 times greater than those of CPFX and pipemidic acid (PPA), respectively. A significant correlation ($r^2 = 0.995$) was achieved between permeability across AM plasma membrane and hydrophobicity, implying that passage through AM membrane was principally involved in the passive diffusion. The extent of AM intracellular binding was the greatest for grepafloxacin, followed by HSR-903, CPFX, levofloxacin and PPA. In conclusion, HSR-903 distributed more efficiently in ELF and AM than CPFX, and the high accumulation of HSR-903 by AM cells may be accounted for by both the high transferability across the AM membrane and avid binding to the membrane phospholipids.

Keywords: Olamufloxacin (HSR-903); Alveolar barrier; Alveolar macrophage; Membrane transport; Phospholipid binding

1. Introduction

Olamufloxacin (HSR-903, Fig. 1) is a newly synthesized oral fluoroquinolone with a broad spectrum of antibacterial activity against Gram-positive and -negative bacteria, atypical organism [1–5]. Accordingly, it has being developed to treat various tissue infections in the clinical development stage, particularly for lower respiratory tract infections.

For many antibacterials, of a great essence is to reach and maintain high concentration (relative to the minimum inhibitory concentration of susceptible pathogens) at the bacterial residing site during most of the dosing intervals in order to optimize the clinical and bacteriological success. It had been demonstrated that AUC ratio of lung to plasma up to 4 h for HSR-903 was 11.0 in rats, 5- to 10-fold higher than those for ciprofloxacin (CPFX) and lomefloxacin [6], respectively. This may be consistent with the good clinical efficacy of HSR-903 in the treatment of the respira-

* Corresponding author. Present address: Department of Pharmaceutics, Hokkaido Pharmaceutical University, 7-1 Katsuraoka-cho, Otaru-city, Hokkaido 047-0264, Japan. Tel./fax: +81 134 62 1848.
E-mail address: morimoto@hokuyakudai.ac.jp (K. Morimoto).

0939-6411/$ - see front matter © 2006 Elsevier B.V. All rights reserved.
doi:10.1016/j.ejpb.2006.04.009

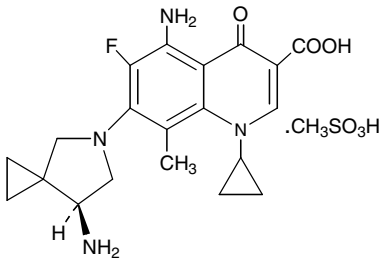

HSR-903

Fig. 1. Chemical structure of HSR-903.

tory tract infections. However, the lung drug concentration may not be precise in elucidating in vivo efficacy response, since drug is unevenly distributed within the lung due to the existence of relatively impermeable barriers. In consequence, the measurement of antibacterial concentrations in the vicinity of pathogens would be more relevant predictor of in vivo antibacterial effectiveness [7]. Within the alveolus compartment, the epithelial lining fluid (ELF), which lies in pools on the inside surface of the alveolus, and the alveolar macrophage (AM), which usually resides in the ELF, are representatively extracellular and intracellular infectious sites in respiratory tract infections, respectively [7].

Depending upon the anatomical and physiological nature of the alveolus, the transfer of drugs from plasma to ELF would encounter the significant alveolar barrier, which consists of three layers, i.e. the lung capillary endothelial cells, the intermediate connective tissue and the alveolar epithelial cells. Such a drug transport characteristic results in the production of a microenvironment for ELF worthy of studying. In addition, drug distribution from ELF to AM would be governed by both AM plasma membrane transport and the binding to the AM intracellular constituents [7]. Therefore, the distribution of HSR-903 in ELF and AM may be considerably different from that in plasma, and should be elucidated in detail.

In the present study, we attempted to investigate the distribution characteristics of orally administered HSR-903 in ELF and AM in rats, and to clarify mechanism underlying the distribution processes from a pharmacokinetic standpoint.

2. Materials and methods

2.1. Materials

HSR-903 and NR-762 (internal standard for HPLC assay) were supplied from Hokuriku Pharm. Co. (Fukui, Japan). Quinidine, propranolol, pipemidic acid (PPA), nalidixic acid and oxolinic acid were purchased from Wako Pure Chem. Co. (Osaka, Japan). ^{3}H-Water (0.037 MBq/μmol) was obtained from Perkin Elmer Life Sciences (Boston, MA). Immobilized artificial membrane (IAM) column (IAM PC.MG, 4.6 mm Ø × 15 cm) was obtained from Regis Technologies, Inc. (Morton Grove, IL). All other reagents were at least of analytical grade.

2.2. Animals

Adult male Wistar rats weighing 200–270 g were purchased from Japan SLC (Shizuoka, Japan). They were housed in a room with controlled temperature and humidity, and had free access to food and water. They were fasted for 20 h before the experiments. All animal studies were performed according to the Guidelines for the Care and Use of Laboratory Animals that was approved by the Committee of Ethics of Animal Experimentation of Hokkaido College of Pharmacy.

2.3. In vivo study

HSR-903 solution was orally administered to rats at a dose of 10 mg/kg. At each predetermined time, rats were anesthetized i.p. with pentobarbital sodium at a dose of 50 mg/kg, blood was collected from the superior vena cava and then immediately sacrificed by exsanguinations from the descending aorta. The trachea was then cannulated and the lungs were lavaged three times with 5 ml of an ice-cold phosphate-buffered saline solution (pH 7.4) containing 1 mM EDTA. The bronchoalveolar lavage (BAL) fluid was immediately centrifuged at 4 °C (650*g* for 10 min) to separate AM cells from the ELF. In order to calculate the antibacterial concentrations in ELF, the apparent volume of ELF was estimated by the method using urea, an endogenous marker of ELF dilution [8]. The mean value estimated in the present study was 395 ± 17 μl/240 g rat. The intracellular volume in AM cells was determined by a velocity-gradient centrifugation technique using ^{3}H-water and was estimated to have a mean value of 4.2 ± 0.3 μl/mg protein [9]. Each time point combined data from six to nine rats, and the whole concentration–time profile was from the different sets of rats.

2.4. Preparation of the cultured AM cells

The AM cells were isolated from rats by the BAL method as described above. The cells were plated at 5×10^5 cells per 2 cm^2 well in a RPMI-1640 medium (Gibco BRL, Life Technologies, Rockville, MD) supplemented with 10% fetal bovine serum (Gibco BRL), 50 μM 2-mercaptoethanol and 10 μg/ml gentamicin. The plate was incubated for 18 h at 37 °C in 95% air + 5% CO_2. The non-adherent cells were removed by washing three times with the RPMI-1640 medium. The viability of cells was routinely checked by the Trypan blue (0.1%, w/v) exclusion test.

2.5. In vitro uptake, efflux and inhibitory study

The AM cells were washed twice with an SFM medium (Gibco BRL), supplemented with 10 mM 2-[4-(2-hydroxyethyl)-1-1-piperazinyl]ethanesulfonic acid (HEPES), and then incubated at 37 °C with the SFM medium containing either HSR-903, PPA, nalidixic acid or oxolinic acid to give

a final concentration in the medium of 500 μM in each case. At the designated time (0–120 min), the medium was removed by aspiration and washed three times with ice-cold PBS. The cells were solubilized for HPLC analysis by the addition of 0.5 ml of 1 N NaOH. Protein concentration in the solubilized cells was measured with Coomassie Protein Assay Reagent (Pierce Chemical Company, Rockford, IL). The stability of quinolone antibacterials in 1 N NaOH solution was checked. No appreciable degradation was observed. Efflux of quinolone antibacterials from AM cells was examined after the cells were incubated for 30 min at 37 °C in an SFM medium containing either HSR-903, CPFX or PPA (each 500 μM). The cells were washed twice with SFM medium and then incubated in the drug-free medium at 37 °C. The amount of a drug remaining in the cells was quantified. Inhibitory effect on HSR-903 uptake by AM was undertaken by incubating cells with SFM medium containing HSR-903 (50 μM) and inhibitors (GPFX, LVFX, quinidine and propranolol, each 2 mM) for 30 min at 37 °C.

2.6. IAM chromatographic conditions and hydrophobicity determination

The extent of binding of drugs to the phospholipid membrane was evaluated using an HPLC system with IAM.PC.MG column, in which the phosphatidylcholine (PhC) is covalently bound to silica via the propylamine group. An aliquot of the drugs, dissolved in PBS (each 100 μM), was injected into the IAM column and the effluent was monitored at the UV wavelength of 215 nm. The mobile phase was composed of 0–30% acetonitrile in a 0.01 M phosphate-buffered saline solution (PBS, pH 7.4). The capacity factor (K'_{IAM}) was calculated as $K'_{\mathrm{IAM}} = (t_{\mathrm{R}} - t_0)/t_0$, where t_{R} and t_0 are the retention times for the test compounds, and a solvent which is not retained by the column to indicate the column dead time, respectively [10]. The K'_{IAM} value was extrapolated to that of a 100% aqueous eluent (expressed as K_{IAM}). Log $D_{\mathrm{O/B,7.4}}$ (hydrophobicity) was determined in an *n*-octanol/buffer system at pH 7.4 according to previously described methods [11].

2.7. Analytical method

The antibacterial concentrations in the plasma, ELF and AM were determined by HPLC. As for HSR-903, briefly, samples of AM, ELF and plasma (0.2 ml) were well mixed with 0.8 ml of 1 M phosphate buffer and 0.1 ml of internal standard NR-762 (1.5 μg/ml). After vortex mixing, the mixtures were extracted by 6 ml organic mixture (CH_3Cl: isopropanol = 9:1) by shaking for 10 min vigorously. After centrifugation at 3000 rpm for 10 min, the 5-ml organic layer was collected and evaporated to dryness at 30 °C under reduced pressure. The resultants were reconstituted in 0.5 ml of 0.1 M citrate buffer (pH 4.0)–acetonitrile (3:1, v/v), and 100 μl of aliquot was subjected to HPLC. The HPLC system consisted of LC-10AD pump (Shimadzu, Kyoto, Japan), RF-10AD UV detector (Shimadzu), CTO-6A column oven (Shimadzu), C-R6A data processing integrator (Shimadzu) and a mighty RP-18 (5 μm, 4.0 × 150 mm, Kanto Chemical Co., Tokyo, Japan). The mobile phase was composed of 0.03 M ammonium phosphate buffer (pH 2.5)–acetonitrile (3:1, v/v). The flow rate was 1.1 ml/min and the eluate was monitored at 308 nm. The peak area ratio vs. concentration in biological samples was linear over the range 0.1–2 μM and the limit of quantification (LOQ) was 0.1 μM. In these conditions, HSR-903 was eluted as a well-defined peak without any interference of contaminants in biological samples. In the case of PPA and other compounds, biological samples were mixed well with a fivefold volume of methanol for deproteinization and then the supernatant was subject to HPLC. A STR ODS-II (5 μm, 4.0 mm × 250 mm, Shinwa Chemical Co., Kyoto, Japan) column was used and eluates were monitored by RF-10AXL fluorescence (Shimadzu) with a flow rate of 0.8 ml/min at 40 °C. The mobile phase, composed of 0.05 M phosphate buffer solution (pH 3)–acetonitrile–methanol (55:20:25, v/v/v), was used to determine nalidixic acid and oxolinic acid [excitation wavelength (λ_{Ex}) of 325 nm and emission wavelength (λ_{Em}) of 366 nm]. The mobile phase of mixture of 0.05 M phosphate buffer solution (pH 3)–acetonitrile–methanol (70:17:13, v/v/v) was used for determining PPA, with $\lambda_{\mathrm{Ex}} = 278$ nm, $\lambda_{\mathrm{Em}} = 448$ nm.

2.8. Pharmacokinetic model

We employed the hybrid pharmacokinetic model in Fig. 3 to describe the distribution of HSR-903 into the alveolus compartment in vivo. The alveolus compartment consisted of ELF and AM. The ELF compartment served as a bridge connecting the blood compartment with the AM compartment, since AM cells usually reside in ELF. The alveolar barrier between blood and ELF was assumed to be a homogeneous single membrane. For this model, it was assumed that lung blood flow was much greater than transport of HSR-903 across the alveolar barrier and that the distribution in the alveolus compartment did not affect the plasma concentration. Therefore, the mass exchange between the plasma compartment and the alveolar compartment was not considered for the analysis of HSR-903 plasma concentrations.

Intestine compartment:

$$\frac{\mathrm{d}X_{\mathrm{a}}}{\mathrm{d}t} = -k_{\mathrm{a}}X_{\mathrm{a}}. \tag{1}$$

Blood compartment:

$$V_1\frac{\mathrm{d}C_{\mathrm{p}}}{\mathrm{d}t} = k_{\mathrm{a}}X_{\mathrm{a}} - k_{10}V_1 f_{\mathrm{p}}C_{\mathrm{p}}. \tag{2}$$

ELF compartment:

$$V_{\mathrm{ELF}}\frac{\mathrm{d}C_{\mathrm{ELF}}}{\mathrm{d}t} = CL_1 f_{\mathrm{p}}C_{\mathrm{p}} + CL_4 f_{\mathrm{T}}C_{\mathrm{AM}} - (CL_2 + CL_3)f_{\mathrm{ELF}}C_{\mathrm{ELF}}. \tag{3}$$

AM compartment:

$$V_{AM}\frac{dC_{AM}}{dt} = CL_3 f_{ELF} C_{ELF} - CL_4 f_T C_{AM}, \quad (4)$$

where X_a is the drug amount in the intestine compartment. C_p, C_{ELF} and C_{AM} are the concentrations in the plasma, ELF and AM cells, respectively. V_1, V_{ELF} and V_{AM} are the volumes of the blood, ELF and AM compartments, respectively. V_{ELF} and V_{AM} are the actual volumes, which were measured in the present study. The parameter k_{10} is the first-order elimination rate constants in the one-compartment model. CL_1 and CL_2 are the influx and efflux clearances, respectively, across the alveolar barrier. CL_3 and CL_4 are the uptake and efflux transport clearances across the AM cell membrane, respectively. The unbound fraction of antibacterials in AM cells, ELF and plasma is defined as f_T, f_{ELF} and f_p. The f_p was 0.45 [6] and f_{ELF} was 0.82 ± 0.03 (measured in this study via ultrafiltration).

The pharmacokinetic modeling to obtain the "best" parameters was performed as judged by an iterative nonlinear least-squares criterion with Akaike's information criterion (AIC) values. The Damping Gauss–Newton method was used for the fitting algorithm. In the first stage, plasma concentrations were fitted to Eqs. (1) and (2) by nonlinear regression analysis using MULTI (RUNGE) [11] to estimate the parameters (k_a, k_{10} and V_1), because the concentration–time profile of HSR-903 in blood was best modeled with single-compartment open model in the pilot study. In the second stage, the plasma profile (C_p) generated by these parameters was used as a forcing function to describe antibacterial concentration in ELF and AM cells, i.e., k_a, k_{10} and V_1 were fixed in the second curve-fitting process. The concentrations of HSR-903 in ELF and AM compartments were fitted to Eqs. (3) and (4) by nonlinear regression analysis to estimate CL_3 and $f_T CL_4$.

The uptake and efflux of antibacterials in the cultured AM cells in vitro were kinetically analyzed according to the same relationship as described by Eq. (4):

$$V_{AM}\frac{dC_{AM}}{dt} = CL_{3,vitro} C_{medium} - CL_{4,vitro} f_T C_{AM}, \quad (5)$$

where $CL_{3,vitro}$ and $CL_{4,vitro}$ are the uptake and efflux clearances across the cultured AM cell membrane in vitro, and C_{medium} represents the antibacterial concentration in the incubation medium. As for efflux process, C_{medium} corresponded to zero. The experimental results shown in Fig. 4A and B were simultaneously fitted to the integral form of Eq. (5) using the program MULTI [12] to estimate $CL_{3,vitro}$ and $f_T CL_{4,vitro}$.

Given that any active transport system does not involve the transport of quinolone antibacterials across the AM cell membrane, $CL_{3,vitro}$ is identical to $CL_{4,vitro}$, and the following relationship can be obtained:

$$\frac{C_{AM}}{C_{medium}} = 1 + \alpha = \frac{1}{f_T}, \quad (6)$$

where α is the binding constant in the AM cell and represents the bound degree of antibacterials within AM cells.

3. Results

3.1. In vivo distribution of HSR-903 in ELF and AM

The concentration–time profiles of HSR-903 in plasma, ELF and AM after 10 mg/kg oral administration of HSR-903 to rats are illustrated in Fig. 2A. The absorption of HSR-903 was relatively rapid, reaching the peak concentration at 0.75 h after oral administration, and then the plasma concentrations decreased mono-exponentially. The HSR-903 concentrations in ELF and AM were remarkably higher than in the plasma (Fig. 2A) and were significantly greater than those of CPFX in Fig. 2B after oral administration [14]. The concentration–time course of HSR-903 in plasma seemed parallel to those in ELF and AM, suggesting the prompt transfer and relatively rapid equilibrium among plasma, ELF and AM. Further-

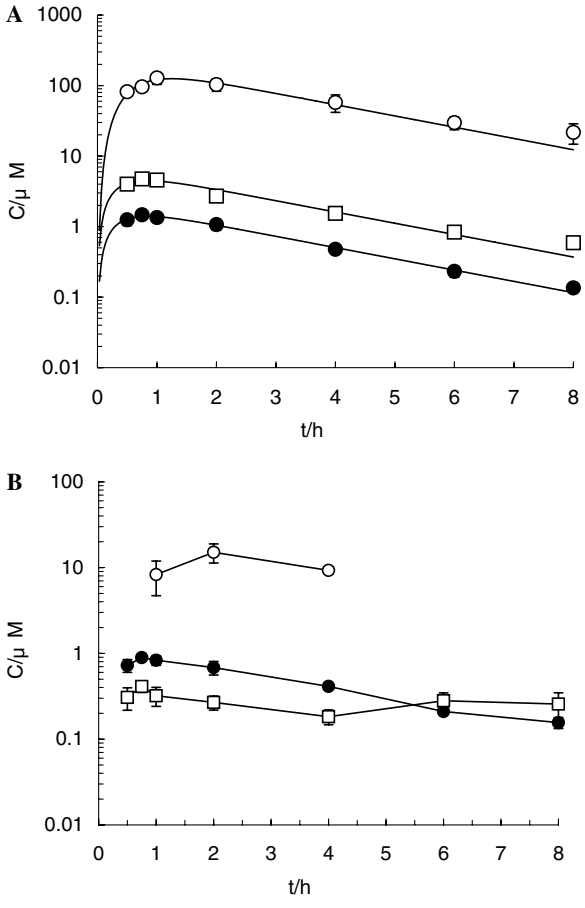

Fig. 2. (A) Concentration–time profiles of HSR-903 in plasma (●), ELF (□) and AM (○). (B) Concentration–time profiles of CPFX [14] in plasma (●), ELF (□) and AM (○). Either HSR-903 or CPFX was orally administered to rats at a dose of 10 mg/kg. Solid lines HSR-903 represent the computer-generated simulation curves using the parameters estimated by the hybrid pharmacokinetic model. Each value represents mean ± S.E. of six to nine rats.

more, the AUC ratio of ELF to plasma of HSR-903 (3.03 ± 0.54, up to 6 h) was around 6.5-fold higher than that of CPFX (0.477 ± 0.075) (Table 1). In addition, the AUC ratio of AM to plasma until 6 h for HSR-903 (97.5 ± 24.2) was approximately 6.5 times greater than that for CPFX (15.1 ± 3.0) (Table 1).

The hybrid pharmacokinetic model of Fig. 3 was suggested to analyze the concentration–time profiles of HSR-903 in plasma, ELF and AM, and was intended to quantitatively evaluate the distribution processes of HSR-903 into ELF and AM. In the case of transfer from blood to ELF, the value of CL_1 (98.46 ± 15.73 ml h^{-1}) was 5.8-fold greater than CL_2 (16.87 ± 3.61 ml h^{-1}), indicative of HSR-903 transport across the alveolar barrier in favor of influx process. In terms of accumulation within AM, the binding constant (α) in vivo was estimated to be approximately 39.6, provided that HSR-903 traverses AM membrane exclusively by passive transport, i.e. $CL_3 = CL_4$. The solid lines drawn in Fig. 2A represented the computer-generated simulation curves using the pharmacokinetic parameters estimated by the present model (Table 2), and were in fairly good agreement with the experimental data (AIC $= -101.3$).

Table 1
AUC ratio for HSR-903 and CPFX distribution into ELF and AM in rats

AUC ratio[a]	HSR-903	CPFX[b]
ELF/plasma	3.03 ± 0.54	0.477 ± 0.075
AM/plasma	97.5 ± 24.2	15.1 ± 3.0

[a] Each AUC ratio is calculated by the trapezoidal method usingthe area under the concentration–time curve, 6 h after oral administration of CPFX or HSR-903 at a dose of 10 mg/kg in rats. Values are expressed as the mean ± S.D.

[b] The CPFX data were performed in the same time as these studies and taken from Ref. [14].

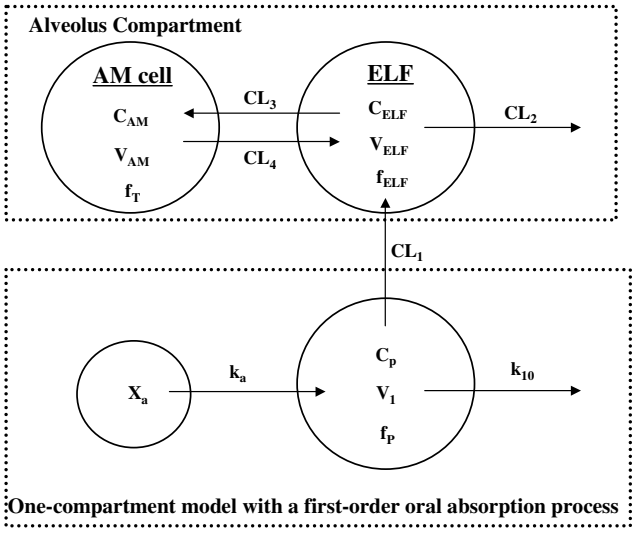

Fig. 3. A hybrid pharmacokinetic model recommended to describe the distribution behavior of HSR-903 into ELF and AM.

Table 2
In vivo pharmacokinetic parameters of HSR-903 in rats

Kinetic parameters	Values
Dose (nmol)	4968 (10 mg/kg)
k_a (h^{-1})	2.78 ± 0.42
K_{10} (h^{-1})	0.82 ± 0.03
V_c (ml)	2501 ± 118
CL_1 (ml h^{-1})	98.46 ± 15.73
CL_2 (ml h^{-1})	16.87 ± 3.61
CL_3 (ml h^{-1})	0.0816 ± 0.0068
$CL_4 f_T$ (ml h^{-1})	0.00206 ± 0.00017

The pharmacokinetic parameters of HSR-903 were estimated using the nonlinear least-squares regression program MULTI (RUNGE) [12] on the basis of rats weighing 240 g. The physiological parameters of V_{ELF} and V_{AM} were estimated as 0.395 and 0.000723 ml/240-g rat, respectively, in separate experiments. Values are expressed as the mean ± S.D.

3.2. In vitro uptake of HSR-903 by the cultured AM cells

Uptake and efflux time profiles for HSR-903, PPA and CPFX were also undertaken in cultured AM cells in vitro,

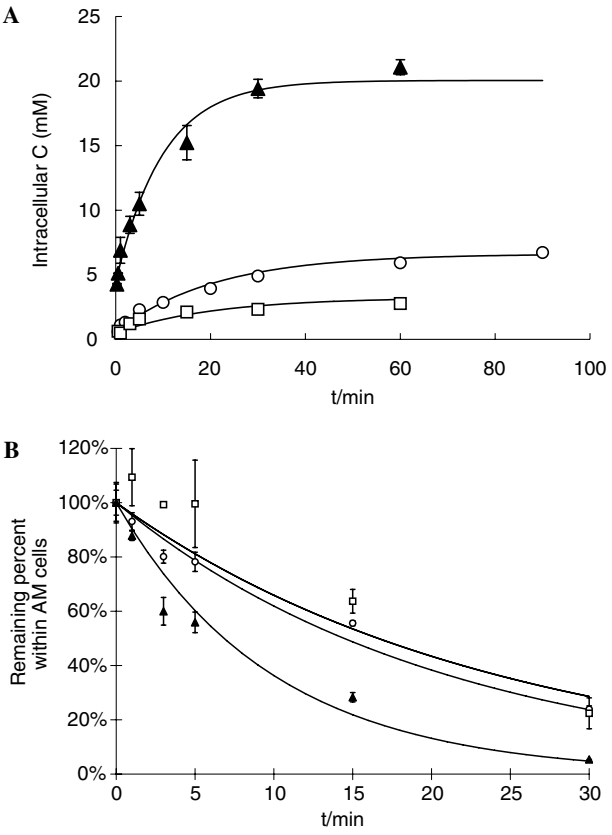

Fig. 4. Time profiles for the uptake (A) and efflux (B) of quinolone antibacterials in cultured AM cells. (A) The cultured AM cells were incubated with medium containing 500 μM HSR-903 (▲), PPA (□) and CPFX (○) at 37 °C for 1–120 min. (B) After AM cells were equilibrated with medium containing 500 μM HSR-903 (▲), PPA (□) or CPFX (○) at 37 °C for 30 min, the cells were washed twice with fresh 37 °C SFM medium, and then incubated in drug-free medium at 37 °C for 1–30 min. Each point represents mean ± S.E. of four to six determinations.

Table 3
Kinetic parameters for membrane transport and intracellular binding in cultured AM cells

Drugs	$CL_{3,vitro}$[a] (μl/min/mg protein)	$f_T CL_{4,vitro}$[a] (μl/min/mg protein)	α[b]	log K_{IAM}[d]	log $D_{O/B,7.4}$[d]
HSR-903	13.3 ± 2.3	0.43 ± 0.07	36.8 ± 1.1	1.28	0.29
PPA	0.92 ± 0.55	0.20 ± 0.11	4.3 ± 0.33	0.12	−1.86
Oxolinic acid	n.d.	n.d.	18.5 ± 0.8	0.64	0.24
Nalidixic acid	n.d.	n.d.	0 ± 0.16	0.14	0.12
GPFX[c]	28.5 ± 4.3	0.67 ± 0.18	44.6 ± 1.43	1.47	0.71
CPFX[c]	2.44 ± 0.20	0.20 ± 0.03	10.7 ± 0.53	0.81	−0.78
LVFX[c]	4.11 ± 0.44	0.77 ± 0.08	6.90 ± 0.12	0.85	−0.46
Quinidine	n.d.	n.d.	50.8 ± 1.9	1.78	2.13
Propranolol	n.d.	n.d.	48.1 ± 1.3	1.91	1.27

n.d. means not determined.
[a] $CL_{3,vitro}$ was estimated by nonlinear least-squares regression analysis of the integral form of Eq. (5) using the program MULTI [13]. Values are the mean ± S.D.
[b] The α values were estimated from Eq. (6). Values are expressed as the mean ± S.E. of four to six determinations.
[c] The data for GPFX, CPFX and LVFX were taken from Ref. [14].
[d] log K_{IAM} represents the binding capacity of drugs to phospholipid membrane and log $D_{O/B,7.4}$ represents drug hydrophobicity. The log K_{IAM} and log $D_{O/B,7.4}$ data were the average of at least three parallel measures.

as shown in Fig. 4A and B. It was evident that the uptake of HSR-903 by AM cells was fast and concentrative at the studied condition. The concentration ratio of HSR-903 in AM cells to in the medium (C_{AM}/C_{medium}), at 60 min after uptake initiation, was 42.1 ± 1.3, which was 3.5- and 7.6-fold higher than those for CPFX (11.9 ± 0.4) and PPA (5.55 ± 0.27), and slightly lower than that of grepafloxacin (GPFX) (55.4 ± 1.4), respectively [14]. In addition, the efflux from AM cells for HSR-903 was fast, and the remaining percentage within the AM cells was 28% for HSR-903, compared to 56% for CPFX and 64% for PPA, respectively, at 15 min after removal of the extracellular drug. Furthermore, the intracellular accumulation of HSR-903 (50 μM) in AM cells was significantly decreased to 57.6 and 60.3%, by 2 mM quinidine and propranolol, respectively. To determine the structural specificity of the AM uptake of HSR-903, the inhibitory effect of several quinolone antibacterial agents was examined. GPFX and LVFX (2 mM) reduced the AM uptake of HSR-903 (50 μM) to 67.9 and 74.4%, respectively.

The uptake and efflux processes of antibacterials in the cultured AM cells in vitro were analyzed from a kinetic standpoint. Depicted in Fig. 4A and B, the solid lines were the generated simulation curves using the pharmacokinetic parameters estimated by the present model (Table 3), which was consistent with experimental results (Fig. 4). The estimated uptake clearance in vitro ($CL_{3,vitro}$) of HSR-903 (13.3 ± 2.3 μl/min/mg protein) was 5.5- and 14.5-fold greater than those of CPFX and PPA, respectively, and was nearly the half compared to GPFX [14]. Moreover, there was a notable correlation observed of $CL_{3,vitro}$ with $D_{O/B,7.4}$ for HSR-903, GPFX, CPFX, LVFX and PPA ($r^2 = 0.995$) (Table 3).

The intracellular binding constant (α) was estimated from the observed C_{AM}/C_{medium} ratio according to Eq. (6). The determined α value in vitro of HSR-903 (36.8 ± 1.1) was comparable to the above-determined α value in vivo (39.6), a little lower than those of GPFX (44.6 ± 1.43) and several fold greater than those of CPFX (10.7 ± 0.53), levofloxacin (LVFX) (6.90 ± 0.12) and PPA (4.3 ± 0.33) (Table 3). In order to evaluate the intracellular binding characteristic, the α values were regressed against either log K_{IAM}, representing the binding capability to immobilized phospholipid membrane, or log $D_{O/B,7.4}$, a hydrophobicity parameter. The α values for HSR-903, GPFX, CPFX, LVFX, PPA, oxolinic acid, nalidixic acid as well as for quinidine and propranolol correlated more significantly with log K_{IAM} ($r^2 = 0.89$) than with log $D_{O/B,7.4}$ ($r^2 = 0.67$).

4. Discussion

The concentration of an antibacterial at the site of infection is generally regarded as a more important factor than in plasma for adequate bacterial killing in order to achieve the effective clinical treatment. Since there exist numerous relatively impermeable barriers in the lung, the distribution for the antibacterials into the infectious sites of lower respiratory tract is challenging. There are several discrete tissue compartments in lung with differing drug concentrations, such as submucosal connective tissue, alveolar epithelium, ELF, AM [14]. The distribution of drugs into each compartment depends upon both the rate of penetration and clearance, and the binding to the specific component within compartments. As for pneumonia, bacteria are chiefly intra-luminal, and ELF and AM appear to be the major locations [14]. The significant alveolar barrier separates ELF from the blood, and the movement of antibacterials from blood into ELF may be accordingly restricted by the alveolar epithelia. In addition, AM cells locate in ELF pool and usually contain the facultative intracellular pathogens [7]. The AM plasma membrane further restricts drug transfer from ELF into AM. Thus, the measurement of antibacterial concentrations in ELF and AM sheds light on the clinical trials efficacy. Besides, the feasibility of sampling ELF and AM was accomplished by the developed BAL method [15].

In this study, we investigated HSR-903 distribution characteristics in ELF and AM in vivo after oral administration to rats, and unveiled that HSR-903 was efficiently distributed in ELF and AM. As shown in Fig. 2, HSR-903 penetrated very readily into ELF and AM, with concentrations reaching 3.23 and 65.5 times greater than that in plasma until 0.75 h. This rapid and pronounced distribution was considered attributable to the good experimental and clinical antibacterial efficacy of HSR-903 in the treatment of lower respiratory infections [5]. The transfer rate of HSR-903 from blood to ELF was marginally faster than to AM. In addition, the pattern of concentration–time course in plasma was analogous to those in ELF and AM after oral administration, suggestive of a swift translocation and rapid equilibration of HSR-903 among plasma, ELF and AM compartments. The phenomenon was also observed for moxifloxacin that the concentration–time curve in plasma was parallel to that in lung tissue after both i.v. and oral administration [16].

As shown in Table 1, the AUC ratio of ELF to plasma of HSR-903 was 3.03 ± 0.54, much higher than a unity. This was in contrast to the free-ligand hypothesis that the unbound concentration in plasma should be equivalent to that in the ELF [17], because the unbound fraction of HSR-903 in plasma and ELF was 0.45 and 0.82, respectively. The possible rationale would be the existence of dissimilar transport capability of HSR-903 at two opposite directions across the alveolar barrier. In addition, the relatively high unbound fraction of HSR-903 in ELF was beneficial to the bacterial killing response in clinic trials.

In terms of the present hybrid pharmacokinetic model, kinetic analyses of the HSR-903 concentration–time curves in ELF and AM illustrated that influx clearance from the plasma to the ELF ($CL_1 = 98.46$ ml/h/240-g rat) was 5.8-fold greater than the efflux clearance from ELF to plasma ($CL_2 = 16.87$ ml/h/240-g rat). In addition, the CL_1 value was much smaller than the lung blood flow (557 ml/h/240-g rats) [18], indicative of the rate-limited step being permeation across the alveolar barrier during HSR-903 transfer from plasma to the ELF. Simultaneously, it pointed to the higher influx than efflux rate across the alveolar barrier in favor of HSR-903 penetration into ELF. To our knowledge, there are several efflux transporters expressed in alveolar epithelia within human and rat lung, including *P*-glycoprotein (i-gp), multidrug resistance-associated protein 1 (MRP1), and breast cancer-resistant protein (BCRP) [19–21]. Additionally, HSR-903 was evidenced to be *P*-gp substrate, and *P*-gp actively participated in HSR-903 efflux from the brain resulting in the restricted brain penetration [22]. In consequence, HSR-903 may undergo the efficient efflux from the alveolar epithelium to the ELF via the ATP-dependent primary active transporters, giving rise to this significant asymmetrical transport.

With respect to transfer into AM, the AUC ratio of AM to plasma for HSR-903 was 97.5 ± 24.2 up to 6 h after the oral administration, nearly 6.5-fold larger than that for CPFX, demonstrating that HSR-903 was highly concentrated in AM cells. In an attempt to clarify the mechanism governing HSR-903 high uptake by AM, the AM cells were isolated from rats and cultured as monolayers in vitro. HSR-903 was found to accumulate concentratively in the cultured AM cells, and C_{AM}/C_{medium} reached 42.1 at 60 min after uptake initiation, several fold higher than those for CPFX and PPA, respectively. Subsequently, uptake and efflux processes of several quinolones were performed, and analyzed kinetically in turn. This in vitro kinetic model consisted of uptake and efflux rate processes conforming to a first-order kinetics, which were described by the clearance dimensions ($CL_{3,vitro}$ and $CL_{4,vitro}$), and the binding to the components within AM cells, which was described as the binding constant (α).

As shown in Fig. 4, the observed concentrations in AM cells for these quinolone antibacterials were in an agreement with the predicted results. The $CL_{3,vitro}$ of HSR-903 (13.3 ± 2.3) across the AM plasma membrane was 5.5 and 14.5 times greater than that of CPFX (2.44 ± 0.20) and PPA (0.92 ± 0.55), respectively. Furthermore, there was excellent correlation between $CL_{3,vitro}$ with $D_{O/B,7.4}$ (hydrophobicity) for HSR-903, GPFX, CPFX, LVFX and PPA, suggesting that the translocation of quinolone antibacterials across AM cell membrane was primarily mediated by passive diffusion. It also agreed that the influx rate into AM cells of quinolones correlated well with lipophilicity [11]. Similarly, trovafloxacin and sparfloxacin were found to passively transverse the human phagocytic cell membrane [23], and the transport of CPFX across human epithelial Calu-3 cells was also via passive diffusion [24].

The estimated α value for HSR-903 (36.8), estimated by Eq. (6), was comparable to the in vivo α value (39.6) (Tables 2 and 3), indicating that the results of kinetic analysis of the in vitro cultured AM cells did reflect the distribution mechanism of HSR-903 in vivo. The α values for quinolone antibacterials as well as quinidine and propranolol correlated better with the respective log K_{IAM} than log $D_{O/B,7.4}$ ($r^2 = 0.89$ vs. 0.67), suggesting that the binding of quinolone antibacterials within AM cells may involve the binding to phospholipids. The forces attributable to partitioning of a solute into IAM surface include both hydrophobic and hydrophilic as well as electrostatic forces, not represented by solutes' hydrophobicity index [25]. This result agreed with good correlation between the extent of binding of GPFX in lung tissue and phosphatidylserine (PhS) contents [26]. Additionally, HSR-903 accumulation by AM cells was significantly inhibited by two amphipathic basic compounds, quinidine and propranolol in this study, both of which were ardently bound to negatively charged phospholipid [26]. Moreover, the binding of HSR-903 to AM membrane phospholipid was also inhibited by the structurally related quinolone analogues, such as GPFX and LVFX. On the other hand, PhC comprised 30.5% of phospholipids contents in the rat AM cells [27]. Therefore, the binding of quinolone antibacterials in the AM cells

should take into consideration the types and quantity of phospholipid components. In addition, the efflux from AM cells for quinolone antibacterials was rapid, reflecting that the binding was not involved in the formation of covalent bond and was reversible. This will be advantageous to the transfer into infectious sites of antibacterials, benefiting from the mobile AM cells serving as drug carrier and reservoir within alveolus space.

In conclusion, it was demonstrated that HSR-903 was efficiently distributed in both ELF and AM, two potential and representative sites for pulmonary infections. In the view of kinetic analysis, there existed the higher influx than efflux clearances across the alveolar barrier in favor of HSR-903 penetration into ELF. Moreover, both rapid permeability across the AM cell membranes and avid binding to the membrane phospholipids were referred to account for the high accumulation of HSR-903 within AM.

References

[1] Y. Niki, N. Miyashita, Y. Kubota, M. Nakajima, T. Matsushima, In vitro and in vivo antichlamydial activities of HSR-903, a new fluoroquinolone antibiotic, Antimicrob. Agents Chemother. 41 (1997) 857–859.

[2] Y. Takahashi, N. Masuda, M. Otsuki, M. Miki, T. Nishino, In vitro activity of HSR-903, a new quinolone Antimicrob, Agents Chemother. 41 (1997) 1326–1330.

[3] H. Tomioka, K. Sato, T. Akaki, H. Kajitani, S. Kawahara, M. Sakatani, Comparative in vitro antimicrobial activities of the newly synthesized quinolone HSR-903, sitafloxacin (DU-6859a), gatifloxacin (AM-1155), and levofloxacin against Mycobacterium tuberculosis and Mycobacterium avium complex, Antimicrob. Agents Chemother. 43 (1999) 3001–3004.

[4] A. Watanabe, Y. Tokue, H. Takahashi, T. Kikuchi, T. Kobayashi, K. Gomi, S. Fujimura, T. Nukiwa, In vitro activity of HSR-903, a new oral quinolone, against bacteria causing respiratory infections, Antimicrob. Agents Chemother. 43 (1999) 1767–1768.

[5] S. Yoshizumi, H. Domon, S. Miyazaki, K. Yamaguchi, In vivo activity of HSR-903, a new fluoroquinolone, against respiratory pathogens, Antimicrob. Agents Chemother. 42 (1998) 785–788.

[6] M. Murata, I. Tamai, Y. Sai, O. Nagata, H. Kato, A. Tsuji, Carrier-mediated lung distribution of HSR-903, a new quinolone antibacterial agent, J. Pharmacol. Exp. Ther. 289 (1999) 79–84.

[7] D.R. Baldwin, D. Honeybourne, R. Wise, Pulmonary disposition of antimicrobial agents: methodological considerations, Antimicrob. Agents Chemother. 36 (1992) 1171–1175.

[8] J.M. Antonini, M.J. Reasor, Accumulation of amiodarone and desethylamiodarone by rat alveolar macrophages in cell culture, Biochem. Pharmacol. 42 (1991) S151–S156.

[9] S.I. Rennard, G. Basset, D. Lecossier, K.M. O'Donnell, P. Pinkston, P.G. Martin, R.G. Crystal, Estimation of volume of epithelial lining fluid recovered by lavage using urea as marker of dilution, J. Appl. Physiol. 60 (1986) 532–538.

[10] Y. Kohno, H. Yoshida, T. Suwa, T. Suga, Uptake of clarithromycin by rat lung cells, Antimicrob. Agents Chemother. 26 (1990) 503–513.

[11] J. Sun, Y. Deguchi, J.M. Chen, R.H. Zhang, K. Morimoto, Interactions between quinolone antibiotics and phospholipid membrane for prediction of alveolar macrophage uptake, Acta Pharmacol. Sin. 23 (2002) 430–438.

[12] K. Yamaoka, T. Nakagawa, A nonlinear least squares program based on differential equations, MULTI (RUNGE), for microcomputers, J. Pharmacobio-Dyn. 6 (1983) 595–606.

[13] K. Yamaoka, Y. Tanigawara, T. Nakagawa, T. Uno, A pharmacokinetic analysis program (MULTI) for microcomputer, J. Pharmacobio-Dyn. 4 (1981) 879–885.

[14] Y. Deguchi, J. Sun, S. Sakai, Y. Tauchi, K. Morimoto, Distribution characteristics of grepafloxacin, a fluoroquinolone antibiotic, in lung epithelial lining fluid and alveolar macrophage, Drug Metab. Pharmacokinet. 18 (2003) 319–326.

[15] P.J. Cook, J.M. Andrews, R. Wise, D. Honeybourn, H. Moudgil, Concentrations of OPC-17116, a new fluoroquinolone antibacterial, in serum and lung compartments, J. Antimicrob. Chemother. 35 (1995) 317–326.

[16] H. Stass, Distribution and tissue penetration of moxifloxacin, Drugs 58 (Suppl. 2) (1999) 229–230.

[17] Y. Deguchi, T. Terasaki, H. Yamada, A. Tsuji, An application of microdialysis to drug tissue distribution study: in vivo evidence for free-ligand hypothesis and tissue binding of β-lactam antibiotics in interstitial fluids, J. Pharmacobio-Dyn. 15 (1992) 79–89.

[18] E. Okezaki, T. Terasaki, M. Nakamura, O. Nagata, H. Kato, A. Tsuji, Structure–tissue distribution relationship based on physiological pharmacokinetics for NY-198, a new antimicrobial agent, and the related pyridonecarboxylic acids, Drug. Metab. Dispos. 16 (1988) 865–875.

[19] L. Campbell, A.G. Abulrob, L.E. Kandalaft, S. Plummer, A.J. Hollins, A. Gibbs, M. Gumbleton, Constitutive expression of *P*-glycoprotein in normal lung alveolar epithelium and functionality in primary alveolar epithelial cultures, J. Pharmacol. Exp. Ther. 304 (2003) 441–452.

[20] A.T. Fojo, K. Ueda, D.J. Slamon, D.G. Poplack, M.M. Gottesman, I. Pastan, Expression of a multidrug resistance gene in human tumors and tissues, Proc. Natl. Acad. Sci USA 84 (1987) 265–269.

[21] G.J.P. Zaman, C.H.M. Versantvoort, J.J.M. Smit, E.W.H.M. Eijdems, M. de Haas, A.J. Smith, H.J. Broxterman, N.H. Mulder, E.G.E. de Vries, F. Baas, P. Borst, Analysis of the expression of MRP, the gene for a new putative transmembrane drug transporter, in human multidrug resistant lung cancer cell lines, Cancer Res. 53 (1993) 1747–1750.

[22] M. Murata, I. Tamai, H. Kato, O. Nagata, A. Tsuji, Efflux transport of a new quinolone antibacterial agent, HSR-903, across the blood–brain barrier, J. Pharmacol Exp. Ther. 290 (1999) 51–57.

[23] A. Pascual, I. Garcia, S. Ballesta, E.J. Perea, Uptake and intracellular activity of trovafloxacin in human phagocytes and tissue-cultured epithelial cells, Antimicrob.Agents Chemother. 41 (1997) 274–277.

[24] M.E. Cavet, M. West, N.L. Simmons, Transepithelial transport of the fluoroquinolone ciprofloxacin: by human epithelial Calu-3 cells, Antimicrob.Agents Chemother. 41 (1997) 2693–2698.

[25] C. Pidgeon, C. Marcus, F. Alvarez, Immobilized artificial membrane chromatography surface chemistry and applications, in: J.W. Kelly, T.O. Baldwin (Eds.), Applications of enzyme Biotechnology, Plenum Press, New York, 1991, pp. 201–220.

[26] T. Suzuki, Y. Kato, H. Sasabe, M. Itose, G. Miyamoto, Y. Sugiyama, Mechanism for the tissue distribution of grepafloxacin, a fluoroquinolone antibiotic, in rats, Drug Metab. Dispos. 30 (2002) 1393–1399.

[27] A. Nishiura, T. Murakami, Y. Higashi, N. Yata, Role of phosphatidylserine in the cellular and subcellular lung distribution of quinidine in rats, Pharm. Res. 5 (1988) 209–213.